bHLH11 negatively regulates Fe homeostasis by its EAR motifs recruiting corepressors in Arabidopsis

Yang Li[a,b,1], Rihua Lei[a,b,1], Mengna Pu[a,b,c], Yuerong Cai[a,b,c], Chengkai Lu[a,b], Zhifang Li[d], Gang Liang[a, b, 2]

[a]CAS Key Laboratory of Tropical Plant Resources and Sustainable Use, Xishuangbanna Tropical Botanical Garden, Chinese Academy of Sciences, Kunming, Yunnan 650223, China

[b]Center of Economic Botany, Core Botanical Gardens, Chinese Academy of Sciences, Menglun, Mengla, Yunnan 666303, China

[c]University of Chinese Academy of Sciences, Beijing 100049, China

[d]State Key Laboratory of Cotton Biology, State Key Laboratory of Crop Stress Adaptation and Improvement, School of Life Sciences, Henan University, No. 85 Minglun Street, Kaifeng, Henan 475001, China

[1]These authors contributed equally to this work

[2]Correspondence: lianggang@xtbg.ac.cn

Running title: bHLH11 acts an active repressor

One-sentence summary: bHLH11 interacts with and inhibits transcriptional activation ability of bHLH IVc TFs via its EAR motifs recruiting the TOPLESS/TOPLESS-RELATED corepressors to finetune Fe homeostasis in Arabidopsis.

ABSTRACT

Iron (Fe) homeostasis is essential for plant growth and development. Although tremendous progress has been made in understanding the maintenance of Fe homeostasis in plants, the underlying molecular mechanisms remain elusive. Recently, bHLH11 was reported to function as a negative regulator. However, the molecular mechanism by which bHLH11 regulates Fe homeostasis is unclear. Here, we generated two *bhlh11* loss-of-function mutants which displayed the enhanced sensitivity to excessive Fe. bHLH11 is located in the cytoplasm and nucleus due to lack of a nuclear location signal sequence, and its interaction partners, bHLH IVc transcription factors (TFs) (bHLH34, bHLH104, bHLH105 and bHLH115) facilitate its nuclear accumulation. bHLH11 exerts its negative regulation function by recruiting the corepressors TOPLESS/TOPLESS-RELATED. Moreover, bHLH11 antagonizes the transactivity of bHLH IVc TFs towards bHLH Ib genes (*bHLH38*, *bHLH39*, *bHLH100* and *bHLH101*). This work indicates that bHLH11 is a crucial component of Fe homeostasis signaling network, playing a pivotal role in the fine-tuning of Fe homeostasis.

INTRODUCTION

Iron (Fe) is an indispensable microelement for plant growth and development. Plants acquire Fe from the soil, which has low concentrations of Fe available, especially in alkaline environments (Jeong and Guerinot, 2009). As about one-third of the world's cultivated land is calcareous (alkaline), iron deficiency is common for plants. Fe functions in many physiological processes, such as photosynthesis, respiration, hormone biosynthesis, and nitrogen fixation. Fe deficiency causes symptoms including delayed growth and leaf chlorosis and can affect the yield and nutritional quality of crops. Although Fe is required for plant growth and development, excess Fe can be toxic to plants because Fe can cause the production of reactive oxygen radicals that are harmful to plant cells (Quinet et al. 2012). Therefore, maintaining Fe homeostasis in plant cells is crucial for their normal growth and development.

Plants have evolved a set of molecular mechanisms for iron absorption, transport, distribution, and storage that ensure appropriate Fe concentrations in cells under low Fe availability. Dicotyledonous and non-gramineous monocotyledonous plants take up Fe using a reduction strategy (strategy I). In *Arabidopsis thaliana*, this strategy involves rhizosphere acidification, ferric iron reduction, and ferrous iron transport. H^+-ATPases such as the P-type ATPase AHA2/AHA7 release protons into the soil, which improves the solubility of Fe in the soil (Santi and Schmidt, 2009; Kobayashi and Nishizawa, 2012).Then, the root surface Fe chelate reductase FERRIC REDUCTION OXIDASE2 (FRO2) catalyzes the reduction of Fe^{3+} to Fe^{2+} (Robinson et al. 1999). Transporters such as IRON-REGULATED TRANSPORTER1 (IRT1) transport Fe^{2+} into roots (Henriques et al. 2002; Varotto et al. 2002; Vert et al. 2002). By contrast, gramineous plants employ a chelation strategy (strategy II) in which high-affinity Fe chelators of the mugineic acid family, also known as phytosiderophores, are secreted into the rhizosphere and facilitate the uptake of the Fe^{3+}-phytosiderophore complex. Recent studies suggest that secretion

of Fe-chelating compounds is also important for the survival of non-gramineous plants such as Arabidopsis in alkaline soil (Rodríguez-Celm et al. 2013; Schmid et al. 2014; Fourcroy et al. 2014; Fourcroy et al. 2016; Siwinska et al. 2018; Tsai et al. 2018).

To maintain Fe homeostasis, plants must sense the environmental Fe concentration and fine-tune the expression of Fe uptake-associated genes accordingly. BRUTUS (BTS) interacts with the basic helix-loop-helix transcription factors bHLH105 and bHLH115 and promotes their degradation (Selote et al. 2015). bHLH105 and bHLH115 belong to the bHLH IVc group, which contains four members. The other two members are bHLH34 and bHLH104. These four members regulate the expression of *FER-LIKE IRON-DEFICIENCY-INDUCED TRANSCRIPTION FACTOR* (*FIT*), bHLH Ib genes (*bHLH38*, *bHLH39*, *bHLH100*, and *bHLH101*) and *POPEYE* (*PYE*) (Zhang et al. 2015; Li et al. 2016; Liang et al. 2017). Recently, three studies characterized the functions of bHLH121 (Kim et al. 2019; Gao et al. 2020; Lei et al. 2020), and Lei et al. (2020) found that *bHLH121* is also directly regulated by bHLH IVc. FIT interacts with bHLH Ib TFs and they synergistically promote the expression of Fe-uptake associated genes *IRT1* and *FRO2* (Yuan et al. 2008; Wang et al. 2013). PYE and bHLH11 are negative regulators of Fe homeostasis (Long et al. 2010; Tanabe et al. 2019). bHLH105/ILR3 also functions as a negative regulator when it interacts with PYE (Tissot et al. 2019). In contrast, bHLH121 is required for activation of numerous Fe deficiency responsive genes (Kim et al. 2019; Gao et al. 2020; Lei et al. 2020). Moreover, both bHLH 121 and PYE interact with bHLH IVc to regulate Fe homeostasis in Arabidopisis (Long et al. 2010; Selote et al. 2015; Kim et al. 2019; Tissot et al. 2019; Gao et al. 2020; Lei et al. 2020). There is also a similar Fe deficiency response signaling network in rice (Ogo et al. 2007; Kobayashi 2013, 2019; Zhang et al. 2017, 2020; Wang et al. 2020; Li et al. 2020).

In the present study, we characterized the roles of bHLH11 in the maintenance of Fe homeostasis in Arabidopsis. bHLH11 recruits the

transcriptional corepressors TOPLESS/TOPLESS-RELATED (TPL/TPR) to exert its transcriptional repression function. bHLH11 is localized in both cytoplasm and nucleus and is exclusively in the nucleus when bHLH IVc TFs are abundant. bHLH11 also interacts with and inhibits bHLH IVc TFs.

RESULTS

Loss-of-function of *bHLH11* impairs Fe homeostasis

Recently, it was reported that the overexpression of *bHLH11* leads to the enhanced sensitivity to Fe deficiency (Tanabe et al. 2019). Here, we also confirmed this result (Figure S1). To further explore the functions of bHLH11, we attempted to isolate two T-DNA insertion mutants from the stocks (WiscDsLoxHs168_11D and SAIL_196_A11). However, no T-DNA was identified within the *bHLH11* gene in the WiscDsLoxHs168_11D; and *bHLH11* mRNA was slightly increased in the homozygous line of SAIL_196_A11 with a T-DNA in the promoter region (data not shown). Although the homozygous line of SAIL_196_A11 was lethal according to the recent study (Tanabe et al. 2019), we observed that they developed as well as the wild type. Thus, we employed the CRISPR-Cas9 system to edit *bHLH11*. Two single guide RNAs were designed to specifically target exons 4 and 3 of *bHLH11* and respectively integrated into the binary vector with a Cas9 (Liang et al. 2016) which were then used for transformation of the wild-type plants. We identified two homozygous mutants (*bhlh11-1* and *bhlh11-2*), the former containing a 1-bp insertion in exon 4 and the latter containing a 2-bp deletion in exon 3 (Figure S2), both of which caused a frameshift mutation in the bHLH domain. When grown on Fe0 or Fe100 media, no visible difference was observed between the *bhlh11* mutants and WT (Figure 1A). By contrast, when grown on Fe300 media, the *bhlh11* mutants produced small shoots (Figure 1A, B). Fe content analysis suggested that the Fe concentration of *bhlh11* mutants was higher

than that of the WT (Figure 1C). These data suggest that the loss-of-function of *bHLH11* leads to the enhanced sensitivity to Fe excess.

To further investigate the effect of bHLH11 on the Fe signaling network, we examined the expression of several Fe homeostasis associated genes (Table 1). *IRT1* and *FRO2* were markedly lower in the *bHLH11-OX* plants than in the WT, whereas *BTS*, *PYE*, (*IRON MAN 1*) *IMA1*, bHLH Ib, were higher. By contrast, *BTS*, *PYE*, *IMA1*, bHLH Ib, and *FIT,* were expressed at higher levels in the *bhlh11* mutants than in the WT. These data suggest that loss-of-function of *bHLH11* impairs Fe homeostasis.

bHLH11 expression and subcellular localization

To investigate the response of *bHLH11* to Fe status, RT-qPCR was used to determine the expression of *bHLH11* in response to Fe status, showing that *bHLH11* mRNA increased in the roots with an increase of Fe concentration in the growth media (Figure 2A), which is in consistence with the recent study (Tanabe et al. 2019). We next examined the response of bHLH11 proteins to Fe status. One-week-old *bHLH11* overexpression plants grown on Fe100 media were transferred to Fe0 or Fe300 media, and root samples were harvested after 1, 2, and 3 days. Immunoblot analysis showed that bHLH11 increased with an increase in Fe concentration and decreased with a decrease in Fe concentration (Figure 2B).

Several Fe-homeostasis associated bHLH TFs were found outside the nucleus (Gratz et al. 2019; Trofimov et al. 2019; Lei et al. 2020; Wang et al. 2020; Liang et al. 2020). To determine the subcellular localization of bHLH11, we generated the 35S:bHLH11-mCherry construct, in which the mCherry tag was fused in frame with the C terminus of bHLH11. When this construct was transiently expressed in tobacco leaves, mCherry was mainly observed in the cytoplasm and nucleus, which is very similar to that of free mCherry (Figure 2C). The cytoplasmic localization of bHLH11 was unexpected because transcription factors are known to function in the nucleus. Thus, we examined

whether bHLH11 can be retained in the cytoplasm due to a lack of a nuclear localization signal (NLS). NLS prediction was conducted by cNLS Mapper with a cutoff score = 4 (Kosugi et al. 2009; http://nls-mapper.iab.keio.ac.jp/cgi-bin/NLS_Mapper_y.cgi). No NLS was found in bHLH11 (Figure S3). When bHLH11 was fused with NLS-mCherry, which contains an NLS from the SV40 virus, bHLH11-NLS-mCherry was exclusively localized in the nucleus (Figure 2C). These data suggest that lack of an NLS causes the cytoplasmic localization of bHLH11.

bHLH11 interacts with bHLH IVc TFs in the nucleus

Considering that TFs usually functions in the nucleus and an NLS allowed bHLH11 to remain in the nucleus, we hypothesized that bHLH11 might be recruited to the nucleus by its nuclear-localized interaction partners. Recent studies revealed that bHLH121, the closest homolog of bHLH11, interacts with bHLH IVc TFs (Kim et al. 2019; Gao et al. 2020; Lei et al. 2020). Therefore, we employed the yeast two-hybrid system to test whether bHLH11 interacts with bHLH IVc TFs. The bHLH11 protein was fused with the GAL4 DNA binding domain in the pGBKT7 vector as the bait (BD-bHLH11). bHLH IVc TFs were cloned to the pGADT7 vector as the preys. As expected, bHLH11 interacts with all four bHLH IVc TFs in yeast (Figure 3A).

To confirm that bHLH IVc TFs interact with bHLH11 in plant cells, we employed the tripartite split-GFP system (Liu et al. 2018). The GFP10 fragment was fused with bHLH IVc proteins in their N-terminus (GFP10-bHLH IVc) and the GFP11 was fused with bHLH11 in the C-terminus (bHLH11-GFP11). When GFP10-bHLH IVc and bHLH11-GFP11 were transiently co-expressed with GFP1-9 in tobacco leaves, the GFP signal was visible in the nucleus of transformed cells (Figure 3B). By contrast, the other combinations did not result in a GFP signal in the cells (Figure 3B).

We next performed a coimmunoprecipitation (Co-IP) assay to confirm the interactions between bHLH IVc TFs and bHLH11 (Figure 3C). MYC tag-fused

bHLH IVc TFs and HA tag-fused bHLH11 were transiently co-expressed in tobacco leaves. The total proteins were incubated with MYC antibody and A/G-agarose beads and then separated on SDS-PAGE for immunoblotting with HA antibody. Consistent with the results from the yeast two-hybrid and tripartite split-GFP assays, bHLH IVc and bHLH11 were present in the same protein complex. These data suggest that bHLH IVc TFs physically interact with bHLH11.

bHLH IVc TFs affect the subcellular localization of bHLH11

Having confirmed that bHLH11 interacts with bHLH IVc TFs in the nucleus, we wondered whether the bHLH IVc TFs have an impact on the subcellular localization of bHLH11. When any one of these four GFP tagged proteins was respectively co-expressed with bHLH11-mCherry, bHLH11-mCherry accumulated exclusively in the nucleus (Figure 4A). By contrast, co-expression of the free GFP did not affect the subcellular localization of bHLH11-mCherry (Figure 4A).

To further confirm the distribution of bHLH11 in the cytoplasm and nucleus, we used immunoblot to measure the expression of the bHLH11 protein. As shown in Figure 4B, bHLH11 protein was detected both in the nucleus and cytoplasm, and both its nuclear and cytoplasmic counterparts were responsive to Fe status.

bHLH11 antagonizes the transactivity of bHLH IVc TFs

The bHLH Ib genes are activated directly by the bHLH IVc TFs (Zhang et al. 2015; Li et al. 2016; Liang et al. 2017). Our expression analyses also suggested that the bHLH Ib genes were upregulated in the *bhlh11* mutants, implying that bHLH11 is a negative regulator of bHLH Ib genes. Because bHLH11 interacts with the bHLH IVc TFs, we proposed that bHLH11 could antagonize the functions of the bHLH IVc TFs. To confirm this hypothesis, transient expression assays were conducted in Arabidopsis protoplasts (Figure

5A). The reporter construct *ProbHLH38:LUC*, in which the LUC reporter was fused with the promoter of *bHLH38,* and different effectors in which the 35S promoter was used to drive GFP, bHLH11 or bHLH IVc, were used in the transient assays. Compared to GFP, bHLH IVc TFs activated the expression of *ProbHLH38:LUC*, whereas bHLH11 had no significant effect. When bHLH11 and bHLH IVc were co-expressed, the the LUC/REN ratio declined significantly. These data suggest that bHLH11 inhibits the transactivity of bHLH IVc TFs towards *bHLH38*.

To further investigate whether bHLH11 inhibits the functions of bHLH IVc TFs by direct protein–protein interaction, we employed the *pGAL4* promoter. In the reporter construct, GFP fused with an NLS sequence was driven by *pGAL4* containing the minimal CaMV 35S promoter with five repeats of the GAL4 binding motif (Figure 5B). In the effectors, the DNA binding domain (BD) of GAL4 was fused in frame with either bHLH104 or bHLH105 and driven by the 35S promoter. Consistent with the fact that bHLH IVc TFs are transcriptional activators, the chimeric BD-bHLH104 or bHLH105 activated the expression of *GFP*. When bHLH11 was co-expressed with BD-bHLH104 or BD-bHLH105, the expression of *GFP* was significantly repressed. These data suggest that bHLH11 antagonizes the transcriptional activation ability of bHLH IVc TFs through direct protein interaction.

Although bHLH11 antagonizes the functions of bHLH IVc TFs, its overexpression caused the increase expression of bHLH Ib genes. We reasoned that the disrupted Fe homeostasis and severe growth inhibition may account for the upregulation expression of bHLH Ib genes in *bHLH11-OX* plants. To confirm our hypothesis, we generated transgenic plants containing a *pER8-bHLH11* construct, in which the *HA-bHLH11* fusion gene was under the control of an inducible promoter, activated by estradiol. Under control conditions, the *bHLH11* transcript level was similar between the WT and *pER8-bHLH11*. After treatment with estradiol, the *bHLH11* gene was overexpressed in the *pER8-bHLH11* plants with no obvious change in the WT

(Figure S4A). As expected, the *pER8-bHLH11* plants displayed enhanced sensitivity to Fe deficiency when gown on Fe0 + estradiol media (Figure S4B). To examine the expression of Fe deficiency-responsive genes, plants grown on Fe100 media were shifted to Fe0 media and Fe0 + estradiol media for 3 days. We found that the expression of bHLH Ib genes was downregulated in the *pER8-bHLH11* plants after treatment with estradiol (Figure 5C).

Taken together, our data suggest that bHLH11 antagonizes the transcriptional activation ability of bHLH IVc TFs.

bHLH11 functions as a transcriptional repressor by recruiting TOPLESS/TOPLESS-RELATED corepressors

Considering that bHLH11 negatively regulated the expression of Fe deficiency-responsive genes, we proposed that bHLH11 is a transcriptional repressor. To investigate how bHLH11 represses transcription, we analyzed its protein sequence and found two typical ethylene-responsive element binding factor-associated amphiphilic repression (EAR) motifs (LxLxL) in the C-terminal region of bHLH11 (Figure 6A;). The EAR motif is a characteristic of proteins interacting with the TPL/TPRs which function as transcription corepressors (Szemenyei et al. 2008; Pauwels et al. 2010; Causier et al. 2012). Thus, we determined whether bHLH11 interacts with TPL/TPRs. Yeast two-hybrid assays indicated that bHLH11 interacts with TPL/TPRs (Figure 6B). To further investigate whether the EAR motifs are required for the interaction, the various EAR-mutated versions, bHLH11m1, bHLH11m2, and bHLH11dm, were tested for the interaction with TPL/TPRs. As shown in Figure 6B, the interaction between bHLH11 and TPL/TPRs was dependent on the EAR motifs, as mutation of both EAR motifs abolished the interaction between bHLH11 and TPL/TPRs.

To investigate whether the EAR motifs are required for the repressor function of bHLH11, we conducted reporter–effector transient expression assays in which bHLH105 was used as an effector to activate

ProbHLH38-LUC. We compared the effects of GFP, bHLH11, bHLH11dm, and bHLH11dm-VP16 (VP16, an established activation domain) on bHLH105 (Figure 6C). Compared to the significant repression effect of bHLH11 on bHLH105, bHLH11dm had no significant effect, whereas bHLH11dm-VP16 enhanced the transactivation function of bHLH105 (Figure 6D). These data suggest that bHLH11 functions as a transcriptional repressor and that this function is dependent on its EAR motifs.

To assess the consequences of disrupting the repressor functions of bHLH11 *in vivo*, we generated *bHLH11dm-VP16* transgenic plants. We hypothesized that *bHLH11dm-VP16* overexpression would not only be able to inhibit the functions of bHLH11 by competing with the endogenous bHLH11, but might also activate the target genes of bHLH11. Indeed, *bHLH11dm-VP16* plants showed enhanced tolerance to Fe deficiency compared to *bHLH11-OX* plants (Figure 6E). Expression analysis suggested that overexpression of *bHLH11dm-VP16* promotes the expression of *IRT1* and *FRO2* (Figure S5). Therefore, the EAR motifs are needed for the repression function of bHLH11.

DISCUSSION

Plants sense Fe-deficient environments and activate a signal transduction cascade that ultimately results in the transcriptional regulation of downstream effector genes of the Fe uptake system. The expression of Fe homeostasis-associated genes is tightly regulated by Fe availability, including environmental Fe availability and local Fe availability in developing tissues and organs. However, this mechanism is not an on-off process but rather a fine-tuned one, with multiple layers of transcription regulations. Considerable progress has been made in deciphering the signal transduction pathways that maintain Fe homeostasis, leading to the identification of many signaling components. Here, we show that bHLH11 acts an active repressor by recruiting TPL/TPRs. bHLH11 contributes to Fe homeostasis through a

sophisticated mechanism that involves physical interaction with bHLH IVc TFs, which down-regulates their transaction activation capacity.

We demonstrated that bHLH11 negatively regulates Fe uptake at the molecular and physiological level. The *bHLH11-OX* plants had reduced Fe concentration whereas its mutants had elevated Fe concentration (Figure 1C; Figure S1D), which is positively correlated with the expression *IRT1* and *FRO2*. It is well known that FIT interacts with bHLH Ib TFs to control the expression of *IRT1* and *FRO2*. Although bHLH Ib genes were upregulated and *FIT* was not affected in the *bHLH11-OX* plants, the expression of *IRT1* and *FRO2* was extremely inhibited (Table 1). Recently, Tanabe et al. (2019) reported that *bHLH11* overexpression inhibits the expression of both *FIT* and *IRT1*/FRO2, and concluded that bHLH11 negatively regulates *IRT1* and *FRO2* in a FIT-dependent manner (Tanabe et al. 2019). However, we did not find the significant response of *FIT* to *bHLH11* overexpression. Therefore, it is plausible that bHLH11 directly represses the expression of *IRT1* and *FRO2*. Recently, Gao et al. (2020) found that bHLH11 interacts with itself in yeast, implying that bHLH11 may function as a homodimer to regulate its target genes.

Two types of transcriptional repressors exist: active and passive (Krogan and Long, 2009). Generally, active repressors repress transcription by recruiting transcriptional repression components, whereas passive repressors indirectly influence transcription by competitively interfering with activators. The TPL/TPRs are a class of corepressors (Causier et al. 2012). Our work confirmed that bHLH11 interacts with TPL/TPRs and negatively regulates gene expression, suggesting that bHLH11 functions as an active repressor. The observation that the EAR motif (LxLxL) is conserved in bHLH11 homologs across different plant species, such as maize (*Zea mays*), rice, and *Brassica rapa* (Figure S6), implies that different plant species employ a conserved repression strategy to fine-tune Fe homeostasis.

The antagonistic regulation between positive and negative transcription

factors is prevalent in plants. For example, the transcription factors MYC2, MYC3, and MYC4 as well as bHLH3, bHLH13, bHLH14, and bHLH17 antagonistically regulate jasmonic acid (JA) signaling (Fernandez-Calvo et al. 2011; Song et al. 2013). In Fe homeostasis signaling, the bHLH IVa TFs (bHLH18, bHLH19, bHLH20, and bHLH25) antagonize the activity of the bHLH Ib TFs in regulating FIT protein stability under Fe deficiency (Cui et al. 2018). Here, we show the antagonistic regulation between bHLH11 and bHLH IVc TFs. In addition to transcriptional regulation, the protein degradation is another type of regulation in Fe homeostasis signaling. As reported previously, bHLH105 and bHLH115 are degraded by BTS via the 26S proteasome pathway (Selote et al. 2015). We found that bHLH11 protein was degraded under Fe deficient conditions (Figure 2B), which may benefit plants by alleviating the repression of bHLH11 to Fe uptake associated genes. These coordinated regulations of transcription and post-transcription may help plants adapt to their various Fe-nutrition habitats.

bHLH11 has no canonical NLS sequence (Figure S3). We showed that bHLH11 exists in the nucleus and cytoplasm and it accumulates in the nucleus with the assistance of its nuclear partners bHLH IVc TFs (Figure 4A). This transcription factor-dependent nuclear localization of bHLH11 might contribute to the maintenance of Fe homeostasis. bHLH11 inhibits the activation ability of bHLH IVc TFs and restricts the expression of Fe uptake-associated genes. The repressor function of bHLH11 may help plants avoid Fe toxicity and adapt to environments with an Fe excess by reducing the rate of Fe uptake. This putative protein shuttling strategy enables plants to respond quickly to Fe fluctuation.

Transcriptional activation of Fe deficiency-responsive genes occurs downstream of the bHLH IVc TFs. However, this mechanism may not be an on–off process. We show that bHLH11 contributes to Fe homeostasis via a sophisticated mechanism. As a negative transcription factor, bHLH11 exerts its repressor function by its EAR motifs recruiting the TPL/TPRs (Figure 6B). On

the other hand, bHLH11 physically interacts with and inhibits bHLH IVc TFs (Figure 5A, B). It is noteworthy the bHLH Ib genes were upregulated in both *bhlh11* mutants and *bHLH11-OX* plants. We hypothesize that a feedback regulation loop exists in the *bHLH11-OX* plants in which the Fe deficiency status caused by *bHLH11* overexpression promotes the upregulation of bHLH Ib genes. Similar feedback regulations are universal in Fe homeostasis. For example, loss-of-function mutations in the Fe transport-associated genes *IRT1*, *FRD3*, or *OPT3* lead to disruption of Fe homeostasis and cause the upregulation of bHLH Ib genes in Arabidopsis (Wang et al. 2007). Therefore, it is likely that the downregulation of *IRT1* and the low Fe status in the *bHLH11-OX* caused the upregulation of bHLH Ib genes by a feedback regulation. In support of this hypothesis, the expression levels of bHLH Ib genes were downregulated in the *pER8-bHLH11* plants after transient treatment with estradiol (Figure 5C), which ruled out the secondary effect caused by constitutive *bHLH11* overexpression.

Therefore, the expression levels of bHLH Ib genes are balanced by both bHLH IVc TFs and bHLH11. This study expands our knowledge of the Fe homeostasis transcription network mediated by bHLH Ib and IVc proteins. Based on our findings, we propose a putative working model for bHLH11 (Figure 7). bHLH11 transcript and protein abundance decrease with a decrease in the environmental Fe concentration. bHLH11 functions as an active repressor by recruiting TPL/TPR corepressors. bHLH11 interacts with and inhibits the transcriptional activation ability of bHLH IVc TFs. When Fe is sufficient or excessive, *bHLH11* transcription is activated and bHLH11 protein accumulates. Some of bHLH11 proteins are recruited by bHLH IVc TFs into the nucleus, where bHLH11 represses the transcription of Fe deficiency-responsive genes by interacting with TPL/TPR corepressors. This enables roots to control Fe uptake and avoid Fe toxicity. Under Fe-deficient conditions, *bHLH11* transcription slows down and bHLH11 protein degradation accelerates, which relieves the repression by bHLH11 to Fe

deficiency-responsive genes and facilitates Fe uptake. Our study provides experimental support for the existence of an elaborate system that allows plants to respond dynamically to Fe status. This mechanism is based on an equilibrium between the activation of Fe uptake-associated genes by bHLH IVc and their repression by bHLH11. Disruption of this equilibrium by misexpression of *bHLH11* disturbs Fe homeostasis. Therefore, bHLH11 is a key component of the Fe homeostasis signaling pathway.

MATERIALS AND METHODS

Plant Materials and Growth Conditions

The *Arabidopsis thaliana* ecotype Columbia-0 was used as the wild type in this study. Plants were grown in long photoperiods (16-hour light/8-hour dark) or short photoperiods (10-hour light/14-hour dark) at 22°C. Surface sterilized seeds were stratified at 4°C for 2 d before being planted on media. Half Murashige and Skoog (MS) media with 1% sucrose, 0.8% agar A and the indicated FeEDTA concentration were used. Fe0 (0 μM Fe), Fe50 (50 μM Fe), Fe100 (100 μM Fe) and Fe300 (300 μM Fe).

Generation of CRISPR/Cas9-edited *bHLH11*

For CRISPR/Cas9-mediated editing of *bHLH11*, two target sites were designed by CRISPR-GE (Xie et al. 2017) to target the third and fourth exon of bHLH11, which were driven by the AtU3b promoter and respectively cloned into the pMH-SA binary vector carrying the Cas9 (Liang et al. 2016). The wild type plants were transformed and positive transgenic plants were selected on half-strength MS medium containing 20 μg/mL hygromycin. The positive transformants were sequenced and the homozygous mutants without hygromycin resistance were selected for further analysis.

Generation of transgenic Plants

HA-tag or VP16 domain were fused in frame with the full-length coding sequence of *bHLH11* to generate *35S:HA-bHLH11* and *35S:bHLH11dm-VP16* in the pOCA30 binary vector. HA-tagged bHLH11 was cloned into pER8 vector (Zuo et al. 2001). These constructs were introduced into Arabidopsis plants using the agrobacterium-mediated floral dip method.

Yeast-two-hybrid assays

Full-length bHLH11 was cloned into pGBKT7 as a bait to screen an iron-depleted cDNA library. The full-length of bHLH IVc in the pGADT7 was described previously (Li et al. 2016). Growth was determined as described in the Yeast Two-Hybrid System User Manual (Clontech).

Subcellular localization

For the construction of *35S:bHLH11-mCherry*, mCherry-tag was fused with bHLH11. *35S:bHLH34-GFP*, *35S:bHLH104-GFP*, *35S:bHLH105-GFP*, *35S:bHLH115-GFP*, and *35S:GFP* were described previously (Lei et al. 2020). *35S:bHLH11-mCherry* was co-expressed with various GFP-containing vectors in tobacco cells. Epidermal cells were recorded on an OLYMPUS confocal microscope. Excitation laser wave lengths of 488 nm and 563 nm were used for imaging GFP and mCherry signals, respectively.

Fluorescence complementation Assays

The tripartite split-GFP fluorescence complementation assay was described as previously (Liu et al. 2018; Lei et al. 2020). bHLH11 was fused with a C-terminal GFP11 tag. The bHLH IVc genes were fused with an N-terminal GFP10 tag. All vectors were introduced into *A. tumefaciens* (strain EHA105) and the various combinations of Agrobacterial cells were infiltrated into leaves of *Nicotiana benthamiana* by an infiltration buffer (0.2 mM acetosyringone, 10 mM $MgCl_2$, and 10 mM MES, PH 5.6). Gene expression was induced 1 day

after agroinfiltration by injecting 20 μM *β*-estradiol in the abaxial side of the leaves. Epidermal cells were recorded on a Carl Zeiss Microscopy.

Co-immunoprecipitation Assay

HA-bHLH11 and MYC-bHLH IVc or MYC-GFP were transiently expressed in the *Nicotiana benthamiana* leaves and the leaves were infiltrated with MG132 12 hours before harvesting. 2 g leaf samples were used for protein extraction in 2 ml IP buffer (50 m M Tris-HCl, pH 7.4, 150 mM NaCl, 1 mM $MgCl_2$, 20% glycerol, 0.2% NP-40, 1 X protease inhibitor cocktail and 1 X phosphatase inhibitor cocktail from Roche). Lysates were clarified by centrifugation at 20, 000 g for 15 min at 4 °C and were immunoprecipitated using MYC antibody. IP proteins were analyzed by immunoblot using anti-HA and anti-MYC antibody respectively (Affinity Biosciences).

Gene Expression Analysis

Total root RNA was extracted by the use of the Trizol reagent (Invitrogen). For the reverse transcription reaction, 1 μg total RNA was used for cDNA synthesis by oligo(dT)18 primer according to the manufacturer's protocol (Takara). The resulting cDNA was subjected to relative quantitative PCR using the ChamQ^{TM} SYBR qPCR Master Mix (Vazyme Biotech Co.,Ltd) on a Roche LightCycler 480 real-time PCR machine, according to the manufacturer's instructions. For gene expression analysis in Arabidopsis plants, *ACT2* was used as an internal control and gene copy number was normalized to that of *ACT2*. For gene expression analysis in tobacco transient expression assays, *NPTII* was used as an internal control and gene copy number was normalized to that of *NPTII*. For the quantification of each gene, three biological replicates were used. The quantitative reverse transcription-PCR primers were listed in Table S1.

Fe Concentration Measurement

To determine Fe concentration, rosette leaves from three-week-old seedlings

grown in soil were harvested and dried at 65 °C for 3 days. For each sample, about 100 mg dry weight was wet-ashed with 1.5 ml of 13.4 M HNO_3 and 1.5 ml of 8.8 M H_2O_2 for 20min at 220°C. Metal concentration was measured using Inductively Coupled Plasma Mass Spectrometry (ICP-MS). Three biological replicates were used for Fe concentration analysis.

Transient expression assays in Arabidopsis protoplasts

Arabidopsis mesophyll protoplasts preparation and subsequent transfection were performed as described previously (Wu et al. 2009). The promoter sequence of *bHLH38* was amplified from genomic DNA and cloned into pGreenII 0800-LUC vector. The coding sequences of GFP and various kinds of bHLHs (bHLH34, bHLH104, bHLH105, bHLH115, bHLH11, bHLH11dm and bHLH11dm-VP16) were respectively cloned into the pGreenII 62-SK vector under control of 35S promoter. For the reporter and effectors, 10 μg plasmid for each construct was used. After protoplasts preparation and subsequent transfection, firefly luciferase (LUC) and renillia luciferase (REN) activities were measured using the Dual-Luciferase Reporter Assay System (Promega) following the manufacturer's instructions. Relative (LUC) activity was calculated by normalizing against the REN activity.

Transient expression assays in Tobacco

Agrobacterium tumefaciens strains EHA105 was used in the transient expression experiments in tobacco. *pGAL4* promoter and BD domain were described previously (Li et al. 2016). *pGAL4* promoter was fused with NLS-GFP and cloned into the pOCA28 binary vector. 35S:BD, 35S:BD-bHLH104, 35S:BD-bHLH105 and 35S:HA-bHLH11 were constructed in the pOCA30 binary vector. For co-infiltration, different agrobacterium strains carrying different constructs were mixed prior to infiltration. Leaf infiltration was conducted in 3-week-old *N. benthamiana*. *NPTII* gene in the pOCA28 vector was used as the internal control. *GFP* transcript abundance was normalized to

that of *NPTII.*

Immunoblotting

For total protein extraction, roots were ground to a fine powder in liquid nitrogen and then resuspended and extracted in RIPA buffer (50 mMTris, 150 mMNaCl, 1% NP-40, 0.5% Sodium deoxycholate, 0.1% SDS, 1 mMPMSF, 1 x protease inhibitor cocktail [pH 8.0]). Isolation of cytoplasmic and nuclear proteins was performed as described previously (Li et al. 2018). Sample was loaded onto 12% SDS-PAGE gels and transferred to nitrocellulose membranes. The membrane was blocked with TBST (10 mM Tris-Cl, 150 mM NaCl, and 0.05% Tween 20, pH8.0) containing 5% nonfat milk (TBSTM) at room temperature for 60 min and incubated with primary antibody in TBSTM (overnight at 4°C). Membranes were washed with TBST (three times for 5 min each) and then incubated with the appropriate horseradish peroxidase-conjugated secondary antibodies in TBSTM at room temperature for 1.5 h. After washing three times, bound antibodies were visualized with ECL substrate.

Supplemental data

Supplemental Figure S1. Phenotypes of *bHLH11-OX* plants.

Supplemental Figure S2. Genotypes of *bhlh11* mutants.

Supplemental Figure S3. Prediction of NLS in bHLH11.

Supplemental Figure S4. Phenotypes of *pER8-bHLH11* transgenic plants.

Supplemental Figure S5. Expression of *IRT1* and *FRO2* in *bHLH11dm-VP16* transgenic plants.

Supplemental Figure S6. Conserved EAR motif in the bHLH11 homologs from various plants species.

Supplemental Table S1. Primers used in this paper.

ACKNOWLEDGEMENTS

We thank the Biogeochemical Laboratory and Central Laboratory (Xishuangbanna Tropical Botanical Garden) for assistance in the determination of metal contents. This work was supported by the National Natural Science Foundation of China (31770270 to Gang Liang).

AUTHOR CONTRIBUTIONS

G.L. conceived the project. Y.L., R.L., M.P., C.L., Z. L., and G.L. constructed plasmids, M.P. and Y.C generated transgenic plants, and Y.L. and R.L. characterized plants, determined gene and protein expression and conducted cellular assays. Y.L. and G.L. wrote the manuscript and all authors discussed and approved the manuscript.

REFERENCES

Causier B, Ashworth M, Guo W, Davies B (2012) The TOPLESS interactome: A framework for gene repression in Arabidopsis. **Plant Physiol** 158: 423-438

Cui Y, Chen CL, Cui M, Zhou WJ, Wu HL, Ling HQ (2018) Four IVa bHLH Transcription Factors Are Novel Interactors of FIT and Mediate JA Inhibition of Iron Uptake in Arabidopsis. **Mol Plant** 11: 1166-1183

Fernandez-Calvo P, Chini A, Fernandez-Barbero G, Chico JM, GimenezIbanez S, et al. (2011) The Arabidopsis bHLH Transcription Factors MYC3 and MYC4 Are Targets of JAZ Repressors and Act Additively with MYC2 in the Activation of Jasmonate Responses. **Plant Cell** 23: 701–715

Fourcroy P, Sisó-Terraza P, Sudre D, Sairón M, Reyt G, Gaymard F, Abadía A, Abadia J, Alvarez-Fernández A, Briat J (2014) Involvement of the ABCG37 transporter in secretion of scopoletin and derivatives by Arabidopsis roots in response to iron deficiency. **New Phytol** 201: 155-167

Fourcroy P, Tissot N, Gaymard F, Briat JF, Dubos C (2016) Facilitated Fe Nutrition by Phenolic Compounds Excreted by the Arabidopsis ABCG37/PDR9 Transporter Requires the IRT1/FRO2 High-Affinity Root Fe(2+) Transport System. **Mol Plant** 9: 485-488

Gao F, Robe K, Bettembourg M, Navarro N, Rofidal V, Santoni V, Gaymard F, Vignols F, Roschzttardtz H, Izquierdo E, Dubos C (2020) The transcription tactor bHLH121 interacts with bHLH105 (ILR3) and its closest homologs to regulate iron homeostasis in Arabidopsis. **Plant Cell** 32: 508-524

Gratz R, Manishankar P, Ivanov R, Köster P, Mohr I, Trofimov K, Steinhorst L, Meiser J, Mai HJ, Drerup M, Arendt S, Holtkamp M, Karst U, Kudla J, Bauer P, Brumbarova T (2019) CIPK11-dependent phosphorylation modulates fit activity to promote arabidopsis iron acquisition in response to calcium signaling. **Dev Cell** 48: 726-740

Tissot N, Robe K, Gao F, Grant-Grant S, Boucherez J, Bellegarde F, Maghiaoui A, Marcelin R (2019) Transcriptional integration of the responses to iron availability in Arabidopsis by the bHLH factor ILR3. **New Phytol** 223:1433-1446

Tsai HH, Rodríguez-Celma J, Lan P, Wu YC, Vélez-Bermúdez IC, Schmidt W. (2018) Scopoletin 8-Hydroxylase-Mediated Fraxetin Production Is Crucial for Iron Mobilization. **Plant Physiol** 177:194-207

Henriques R, Jásik J, Klein M, Martinoia E, Feller U, Schell J, Pais MS, Koncz C (2002) Knock-out of Arabidopsis metal transporter gene IRT1 results in iron deficiency accompanied by cell differentiation defects. **Plant Mol Biol** 50: 587–597

Jeong J, Guerinot ML. (2009) Homing in on iron homeostasis in plants. Trends **Plant Sci** 14: 280-285

Kagale S, Links MG, Rozwadowski K (2010) Genome-wide analysis of Ethylene responsive element binding factor-associated Amphiphilic Repression motif-containing transcriptional regulators in Arabidopsis. **Plant Physiol** 152: 1109-1134

Kim SA, LaCroix IS, Gerber SA, Guerinot ML. (2019) The iron deficiency response in Arabidopsis thaliana requires the phosphorylated transcription factor URI. **Proc Natl Acad Sci USA** 116: 24933-24942

Kosugi S, Hasebe M, Tomita M, Yanagawa H (2009) Systematic identification of yeast cell cycle-dependent nucleocytoplasmic shuttling proteins by prediction of composite motifs. **Proc Natl Acad Sci USA** 106**:** 10171-10176

Krogan NT, Long JA (2009) Why so repressed? Turning off transcription during plant growth and development. **Curr Opin Plant Biol** 12: 628-636

Kobayashi T, Nishizawa NK (2012) Iron uptake, translocation, and regulation in higher plants. **Annu Rev Plant Biol** 63: 131–152

Kobayashi T, Ozu A, Kobayashi S, An G, Jeon JS, Nishizawa NK (2019) OsbHLH058 and OsbHLH059 transcription factors positively regulate iron deficiency responses in rice. **Plant Mol Biol** 101: 471-486

Lei R, Li Y, Cai Y, Li C, Pu M, Lu C, Yang Y, Liang G (2020) bHLH121 Functions as a Direct Link that Facilitates the Activation of FIT by bHLH IVc Transcription Factors for Maintaining Fe Homeostasis in Arabidopsis. **Mol Plant** doi: 10.1016/j.molp.2020.01.006

Li C, Liu X, Qiang X, Li X, Li X, Zhu S, Wang L, Wang Y, Liao H, Luan S, Yu F (2018) EBP1 nuclear accumulation negatively feeds back on FERONIA-mediated RALF1 signaling. **PLoS Biol** 16(10):e2006340

Li X, Zhang H, Ai Q, Liang G, Yu D (2016) Two bHLH transcription factors, bHLH34 and bHLH104, regulate iron homeostasis in *Arabidopsis thaliana*.

Plant Physiol 170: 2478-2493

Liang G, Zhang HM, Lou DJ, Yu DQ (2016) Selection of highly efficient sgRNAs for CRISPR/Cas9-based plant genome editing. **Sci Rep** 6: 21451

Liang G, Zhang HM, Li XL, Ai Q, Yu D (2017) bHLH transcription factor bHLH115 regulates iron homeostasis in Arabidopsis thaliana. **J Exp Bot** 68: 1743-1755

Liang G, Zhang H, Li Y, Pu M, Yang Y, Li C, Lu C, Xu P, Yu D (2020) Oryza sativa Fer-like fe deficiency-induced transcription factor (OsFIT/OsbHLH156) interacts with OsIRO2 to regulate iron homeostasis. **J Integr Plant Biol** doi: 10.1111/jipb.12933.

Liu L, Zhang Y, Tang S, Zhao Q, Zhang Z, Zhang H, Dong L, Guo H, Xie Q (2010) An efficient system to detect protein ubiquitination by agroinfiltration in Nicotiana benthamiana. **Plant J** 61: 893-903

Liu TY, Chou WC, Chen WY, Chu CY, Dai CY, Wu PY (2018) Detection of membrane protein-protein interaction in planta based on dual-intein-coupled tripartite split-GFP association. **Plant J** 94: 426-438

Long TA, Tsukagoshi H, Busch W, Lahner B, Salt DE, Benfey PN (2010) The bHLH transcription factor POPEYE regulates response to iron deficiency in Arabidopsis roots. **Plant Cell** 22: 2219-2236.

Ogo Y, Itai RN, Nakanishi H, Kobayashi T, Takahashi M, Mori S, Nishizawa NK (2007) The rice bHLH protein OsIRO2 is an essential regulator of the genes involved in Fe uptake under Fe-deficient conditions. **Plant J** 51: 366-377

Pauwels L, Barbero GF, Geerinck J, Tilleman S, Grunewald W, Pérez AC, Chico JM, Bossche RV, Sewell J, Gil E, García-Casado G, Witters E, Inzé D, Long JA, De Jaeger G, Solano R, Goossens A. (2010) NINJA connects the co-repressor TOPLESS to jasmonate signalling. **Nature** 464:788-791

Quinet M, Vromman D, Clippe A, Bertin P, Lequeux H, Dufey I, Lutts S, Lefèvre I (2012) Combined transcriptomic and physiological approaches reveal strong differences between short- and long-term response of rice (Oryza sativa) to iron toxicity. **Plant Cell Environ** 35:1837–1859

Robinson NJ, Procter CM, Connolly EL, Guerinot ML (1999) A ferricchelate reductase for iron uptake from soils. **Nature** 397: 694–697

Rodríguez-Celma J, Lin W-D, Fu G-M, Abadía J, López-Millán, Schmidt W (2013) Mutually exclusive alterations in secondary metabolism are critical for the uptake of insoluble iron compounds by Arabidopsis and Medicago truncatula. **Plant Physiol** 162: 1473-1485

Samira R, Li B, Kliebenstein D, Li C, Davis E, Gillikin JW, Long TA. (2018). The bHLH transcription factor ILR3 modulates multiple stress responses in Arabidopsis. **Plant Mol Biol** 97: 297-309

Santi S, Schmidt W (2009) Dissecting iron deficiency-induced proton extrusion in Arabidopsis roots. **New Phytol** 183: 1072–1084

Selote D, Samira R, Matthiadis A, Gillikin JW, Long TA (2015) Iron-binding E3 ligase mediates iron response in plants by targeting basic helix-loop-helix transcription factors. **Plant Physiol** 167: 273-286

Schmid NB, Giehl RF, Döll S, Mock HP, Strehmel N, Scheel D, Kong X, Hider RC, von Wirén (2014) Feruloyl-CoA 69-Hydroxylase1-dependent coumarins mediate iron acquisition from alkaline substrates in Arabidopsis. **Plant Physiol** 164: 160-172

Shahbazian MD, Grunstein M (2007) Functions of site-specific histone acetylation and deacetylation. **Annu Rev Biochem** 76:75-100

Siwinska J, Siatkowska K, Olry A, Grosjean J, Hehn A, Bourgaud F, Meharg AA, Carey M, Lojkowska E, Ihnatowicz A (2018) Scopoletin 8-hydroxylase: a novel enzyme involved in coumarin biosynthesis and iron-deficiency responses in Arabidopsis. **J Exp Bot** 69:1735-1748

Song S, Qi T, Fan M, Zhang X, Gao H, Huang H, Wu D, Guo H, Xie D (2013) The bHLH subgroup IIId factors negatively regulate jasmonate-mediated plant defense and development. **PLoS Genet** 9(7):e1003653

Szemenyei H, Hannon M, Long JA (2008) TOPLESS mediates auxi dependent transcriptional repression during Arabidopsis embryogensis. **Science** 319: 1384-138

Tanabe N, Noshi M, Mori D, Nozawa K, Tamoi M, Shigeoka S. (2019) The basic helix-loop-helix transcription factor, bHLH11 functions in the iron-uptake system in Arabidopsis thaliana. **J Plant Res** 132: 93-105

Tissot N, Robe K, Gao F, Grant-Grant S, Boucherez J, Bellegarde F, Maghiaoui A, Marcelin R, Izquierdo E, Benhamed M, Martin A, Vignols F1, Roschzttardtz H, Gaymard F, Briat JF, Dubos C (2019) Transcriptional integration of the responses to iron availability in Arabidopsis by the bHLH factor ILR3. **New Phytol** 223:1433-1446

Trofimov K, Ivanov R, Eutebach M, Acaroglu B, Mohr I, Bauer P, Brumbarova T. (2019) Mobility and localization of the iron deficiency-induced transcription factor bHLH039 change in the presence of FIT. **Plant Direct** 3(12):e00190

Wang HY, Klatte M, Jakoby M, Bäumlein H, Weisshaar B, Bauer P (2007) Iron deficiency-mediated stress regulation of four subgroup Ib BHLH genes in Arabidopsis thaliana. **Planta** 226: 897-908

Wang N, Cui Y, Liu Y, Fan H, Du J, Huang Z, Yuan Y, Wu H, Ling HQ (2013) Requirement and functional redundancy of Ib subgroup bHLH proteins for iron deficiency responses and uptake in Arabidopsis thaliana. **Mol Plant** 6: 503-513

Wang S, Li L, Ying Y, Wang J, Shao JF, Yamaji N, Whelan J, Ma JF, Shou H (2020) A transcription factor OsbHLH156 regulates Strategy II iron acquisition through localising IRO2 to the nucleus in rice. **New Phytol** 225:1247-1260

Wu FH, Shen SC, Lee LY, Lee SH, Chan MT, Lin CS (2009) Tape-Arabidopsis Sandwich - a simpler Arabidopsis protoplast isolation method. **Plant Methods** 5:16

Yuan Y, Wu H, Wang N, Li J, Zhao W, Du J, Wang D, Ling HQ (2008) FIT interacts with AtbHLH38 and AtbHLH39 in regulating iron uptake gene expression for iron homeostasis in Arabidopsis. **Cell Res** 18: 385–397

Zhang H, Li Y, Yao X, Liang G, Yu D (2017) POSITIVE REGULATOR OF IRON

HOMEOSTASIS1, OsPRI1, facilitates iron homeostasis. **Plant Physiol** 175: 543-554

Zhang J, Liu B, Li M, Feng D, Jin H, Wang P, Liu J, Xiong F, Wang J, Wang HB (2015) The bHLH Transcription Factor bHLH104 Interacts with IAA-LEUCINE RESISTANT3 and Modulates Iron Homeostasis in Arabidopsis. **Plant Cell** 27: 787-805

Zheng L, Ying Y, Wang L, Wang F, Whelan J, Shou H (2010) Identification of a novel iron regulated basic helix-loop-helix protein involved in Fe homeostasis in Oryza sativa. **BMC Plant Biol** 10:166

Zuo J, Niu QW, Chua NH (2001) Technical advance: An estrogen receptor-based transactivator XVE mediates highly inducible gene expression in transgenic plants. **Plant J** 24: 265-273

iency responsive genes in WT, *bHLH11-OX* plants and *bhlh11* mutants.

Fe100			Fe0				
-24	*bhlh11-1*	*bhlh11-2*	WT	*OX-20*	*OX-24*	*bhlh11-1*	*bhlh11-2*
9±0.02^{b}	1.82±0.22^{c}	1.65±0.17^{c}	59.72±2.61^{A}	0.33±0.07^{A}	0.38±0.04^{A}	75.09±2.64^{C}	70.21±1.30^{C}
2±0.04^{b}	1.29±0.05^{c}	1.51±0.15^{c}	69.28±1.80^{C}	0.49±0.04^{A}	0.52±0.05^{A}	98.37±3.64^{C}	97.06±8.66^{C}
7±0.25^{c}	3.48±0.23^{b}	3.62±0.13^{b}	80.79±2.32^{A}	106.52±4.12^{B}	94.5±4.63^{B}	96.04±1.82^{B}	97.28±3.71^{B}
3±0.57^{c}	2.62±0.57^{b}	3.00±0.14^{b}	43.06±3.33^{A}	61.67±2.36^{B}	61.28±0.82^{B}	64.08±2.56^{B}	62.48±4.31^{B}
9±0.92^{c}	2.04±0.15^{b}	2.31±0.24^{b}	72.87±2.72^{A}	105.75±3.00^{B}	101.34±0.89^{B}	102.64±2.38^{B}	97.54±2.48^{B}
7±0.49^{b}	1.33±0.23^{a}	1.35±0.25^{a}	41.01±1.94^{A}	58.65±3.83^{B}	68.15±1.67^{C}	65.09±4.20^{BC}	67.5±2.98^{C}
.7±0.20^{a}	1.05±0.08^{a}	1.04±0.05^{a}	3.12±0.12^{A}	3.21±0.11^{A}	3.10±0.14^{A}	3.07±0.24^{A}	3.00±0.11^{A}
5±0.24^{c}	2.64±0.49^{b}	3.48±0.63^{bc}	5.29±0.30^{A}	7.00±0.13^{BC}	7.82±0.41^{C}	6.21±0.10^{B}	6.59±0.63^{B}
0±0.19^{c}	1.53±0.22^{b}	1.30±0.23^{ab}	3.34±0.28^{A}	4.18±0.15^{B}	4.56±0.46^{B}	4.55±0.43^{B}	5.04±0.25^{B}
5±0.30^{b}	1.52±0.19^{b}	1.47±0.22^{b}	5.65±1.00^{C}	61.03±6.82^{D}	69.3±5.64^{D}	8.43±0.55^{C}	9.5±1.46^{C}
9±0.16^{a}	1.05±0.07^{a}	1.22±0.17^{a}	1.97±0.18^{A}	2.12±0.20^{A}	2.02±0.12^{A}	2.20±0.21^{A}	2.17±0.29^{A}
0±0.41^{a}	1.16±0.26^{a}	1.29±0.37^{a}	5.41±0.57^{AB}	5.80±1.32^{B}	6.00±1.75^{B}	4.96±0.29^{A}	6.26±0.71^{B}
.5±0.25^{a}	0.95±0.18^{a}	0.99±0.29^{a}	2.91±0.14^{A}	4.01±0.40^{B}	3.23±0.28^{B}	3.89±0.21^{B}	3.85±0.27^{B}
6.06±10.71^{c}	1.07±0.06^{a}	1.10±0.09^{b}	0.52±0.04^{B}	111.79±8.64^{C}	125.71±7.98^{C}	0.49±0.02^{A}	0.54±0.07^{A}

Fe0 media for 7d. RNA was prepared from root tissues. The expression of *ACT2* was used to normalize mRNA levels, and the gene 100 was set to 1^{a}. Different letters above each bar indicate statistically significant differences as determined by one-way ANOVA parison test ($P < 0.05$) and .

Figure Legends

Figure 1. *bhlh11* loss-of-function mutants are sensitive to excessive Fe.

(A) Phenotypes of *bhlh11* mutants. Two-week-old seedlings grown on Fe0, Fe100 or Fe300 media.

(B) Shoot biomass of *bhlh11* mutants. Fresh weight of two-week-old shoots grown on Fe0, Fe100 or Fe300 media. Student' t test indicated that the values marked by an asterisk are significantly different from the corresponding wild-type value ($P < 0.05$).

(C) Fe concentration of rosette leaves of 3-week-old WT and *bhlh11* plants grown in soil. Student' t test indicated that the values marked by an asterisk are significantly different from the corresponding wild-type value ($P < 0.05$).

Figure 2. Response of bHLH11 to Fe status

(A) RT-qPCR analysis of *bHLH11* expression. Four-day-old plants grown on Fe100 media were shifted to Fe0, Fe50, Fe100, and F300 media for 3 days. Roots were used for RNA extraction and RT-qPCR. The different letters above each bar indicate statistically significant differences as determined by one-way ANOVA followed by Tukey's multiple comparison test ($P < 0.05$).

(B) Degradation of bHLH11 in response to Fe deficiency. Seven-day-old WT and *bHLH11-OX-20* seedlings grown on Fe100 media were transferred to Fe0 or Fe300 media, and root samples were harvested after 1, 2, and 3 days. anti-HA was used to detect HA-bHLH11. β-tubulin was detected by anti-β-tubulin and used as a loading control.

(C) Subcellular localization of bHLH11. The free mCherry, bHLH11-mCherry or bHLH11-NLS-mCherry were transiently expressed in tobacco leaves.

Figure 3. bHLH11 physically interacts with bHLH IVc TFs.

(A) Yeast two-hybrid analysis of the interaction between bHLH11 and bHLH IVc TFs. Yeast cotransformed with different BD and AD plasmid combinations

was spotted on synthetic dropout medium lacking Leu/Trp (SD–W/L) or Trp/Leu/His/Ade (SD –W/L/H/A).

(B) Interaction of bHLH11 and bHLH IVc TFs in plant cells. Tripartite split-sfGFP complementation assays were performed. bHLH34, bHLH104, bHLH105, and bHLH115 were fused with GFP10, and bHLH11 was fused with GFP11. The combinations indicated were introduced into Agrobacterium and co-expressed in *Nicotiana benthamiana* leaves..

(C) Co-IP analysis of the interaction between bHLH11 and bHLH IVc TFs. Total proteins from different combinations of HA-bHLH11 and MYC-GFP, MYC-bHLH34, MYC-bHLH104, MYC-bHLH105, or MYC-bHLH115 were immunoprecipitated with anti-MYC followed by immunoblotting with the indicated antibodies. MYC-GFP was used as the negative control. Protein molecular weight (in kD) is indicated to the left of the immunoblot.

Figure 4 Change of bHLH11 subcellular localization.

(A) Location of bHLH11 in the absence or presence of bHLH IVc. bHLH11-mCherry was co-expressed with bHLH IVc TFs. The combination of bHLH11-GFP and free mCherry was used as a negative control. Transient expression assays were performed in tobacco leaves.

(B) Immunoblot analysis of bHLH11 protein distributions in the cytoplasm and nuclear fractions. Seven-day-old *bHLH11-OX-20* seedlings grown on Fe100 media were transferred to Fe0 or Fe300 media. Root samples were harvested after 3 days, and cytoplasmic and nuclear proteins were extracted and subjected to immunoblot analysis with the indicated antibodies.

Figure 5. bHLH11 antagonizes the transcriptional activation ability of bHLH IVc TFs.

(A) bHLH11 represses the functions of bHLH IVc TFs. Schematic diagram of the constructs transiently expressed in Arabidopsis protoplasts. The LUC/REN ratio represents the LUC activity relative to the internal control (REN driven by

the 35S promoter). The asterisk indicates a significant difference as determined by Students' t test.

(B) bHLH11 inhibits the functions of bHLH IVc TFs by direct protein–protein interaction. The schematic diagram shows the constructs used in the transient expression assays in tobacco leaves. The abundance of *GFP* was normalized to that of *NPTII*. The asterisk indicates a significant difference as determined by Students' t test.

(C) Expression of bHLH Ib genes in *pER8-bHLH11* plants. Seven-day-old plants grown on Fe0 media were transferred to Fe0 media with or without 4 μM estradiol for 6 h, and root samples were harvested and used for RNA extraction and RT-qPCR. The different letters above each bar indicate statistically significant differences as determined by one-way ANOVA followed by Tukey's multiple comparison test ($P < 0.05$).

Figure 6. bHLH11 acts as a repressor by recruiting TPL/TPR corepressors.

(A) Schematic diagram of the various mutated versions of bHLH11. The mutated amino acid is indicated in red. bHLH11m1, the first EAR mutated. bHLH11m2, the second EAR mutated. bHLH11dm, both double EARs mutated. bHLH11dm-VP16, bHLH11dm fused with the VP16 domain.

(B) The EAR motifs are required for the interaction between bHLH11 and TPL/TPR. Yeast cotransformed with different BD and AD plasmid combinations was spotted on synthetic dropout medium lacking Leu/Trp (SD –T/L) or Trp/Leu/His/Ade (SD –T/L/H/A).

(C) The schematic diagram shows the constructs used in the transient expression assays in (D).

(D) The EAR motifs are required for the repression of bHLH11. Arabidopsis protoplasts were used for transient expression assays.

(E) Phenotypes of *bHLH11dm-VP16* and *bHLH11-OX* plants. Seven-day-old seedlings grown on Fe0 or Fe100 media are shown.

Figure 7. A working model of bHLH11 in Fe homeostasis.

bHLH11 functions as an active repressor by recruiting TPL/TPR corepressors Under Fe-sufficient conditions, *bHLH11* message is activated and its protein accumulates. bHLH11 inhibits the transactivity of bHLH IVc TFs to bHLH Ib genes. bHLH11 may directly regulate the expression of Fe deficiency-responsive gene *IRT1* and *FRO2* (as indicated by a question sign). The repressor function of bHLH11 allows plants to avoid Fe toxicity. Under Fe-deficient conditions, unknown proteins repress the transcription of *bHLH11*, which alleviates the bHLH11-mediated repression to bHLH IVc TFs. bHLH IVc TFs promotes the transcription of bHLH Ib genes. bHLH Ib TFs and FIT activate the expression of the Fe uptake-associated gene *IRT1* and *FRO2*. The question signs indicate unknown proteins.

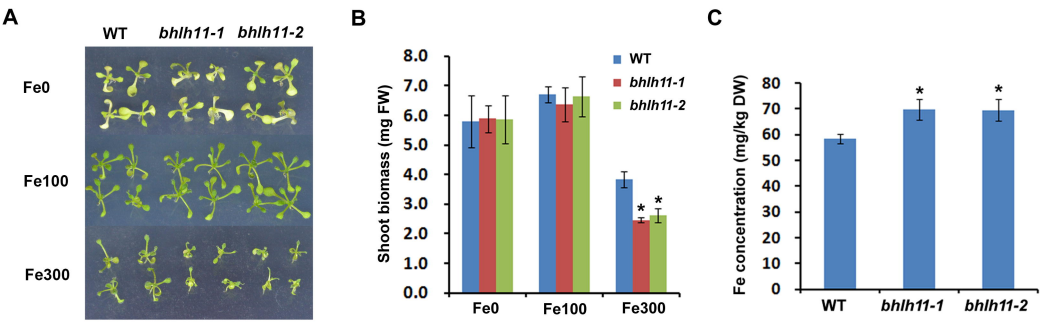
A
WT
bhlh11-1
bhlh11-2
Fe0
Fe100
Fe300
B
Shoot biomass (mg FW)
8.0
7.0
6.0
5.0
4.0
3.0
2.0
1.0
0.0
WT
bhlh11-1
bhlh11-2
*
*
Fe0
Fe100
Fe300
C
Fe concentration (mg/kg DW)
80
70
60
50
40
30
20
10
0
*
*
WT
bhlh11-1
bhlh11-2

A

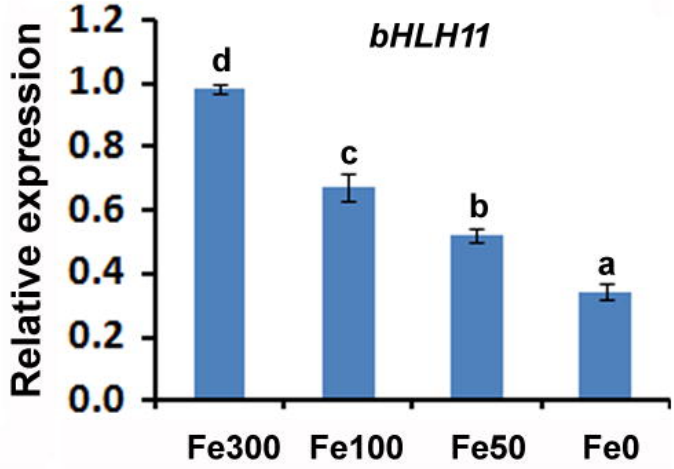
bHLH11
Relative expression
1.2
1.0
0.8
0.6
0.4
0.2
0.0
d
c
b
a
Fe300
Fe100
Fe50
Fe0

B

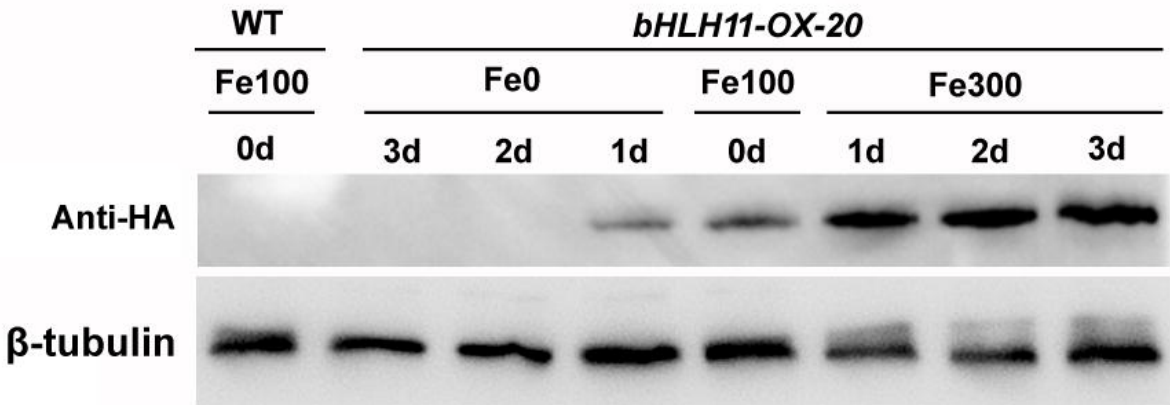
WT
bHLH11-OX-20
Fe100
Fe0
Fe100
Fe300
0d
3d
2d
1d
0d
1d
2d
3d
Anti-HA
β-tubulin

C

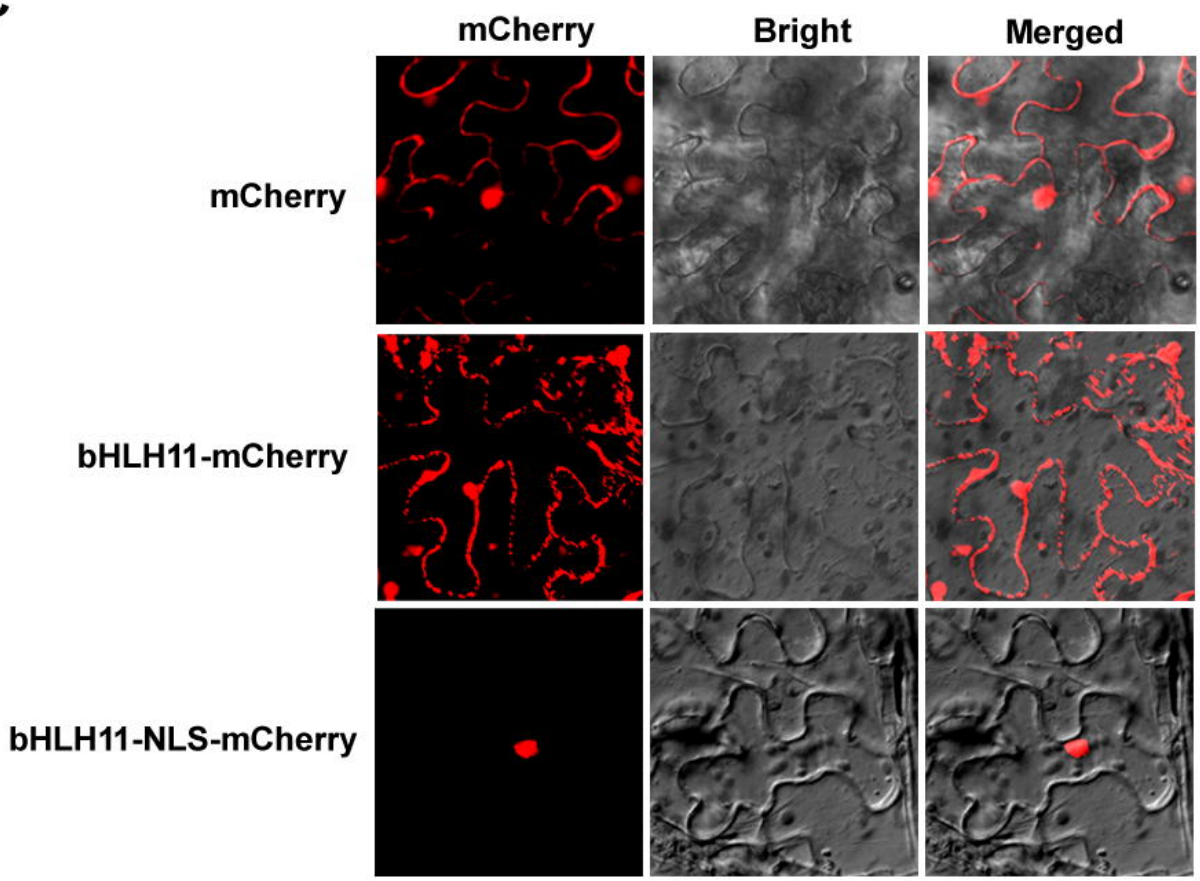
mCherry
Bright
Merged
mCherry
bHLH11-mCherry
bHLH11-NLS-mCherry

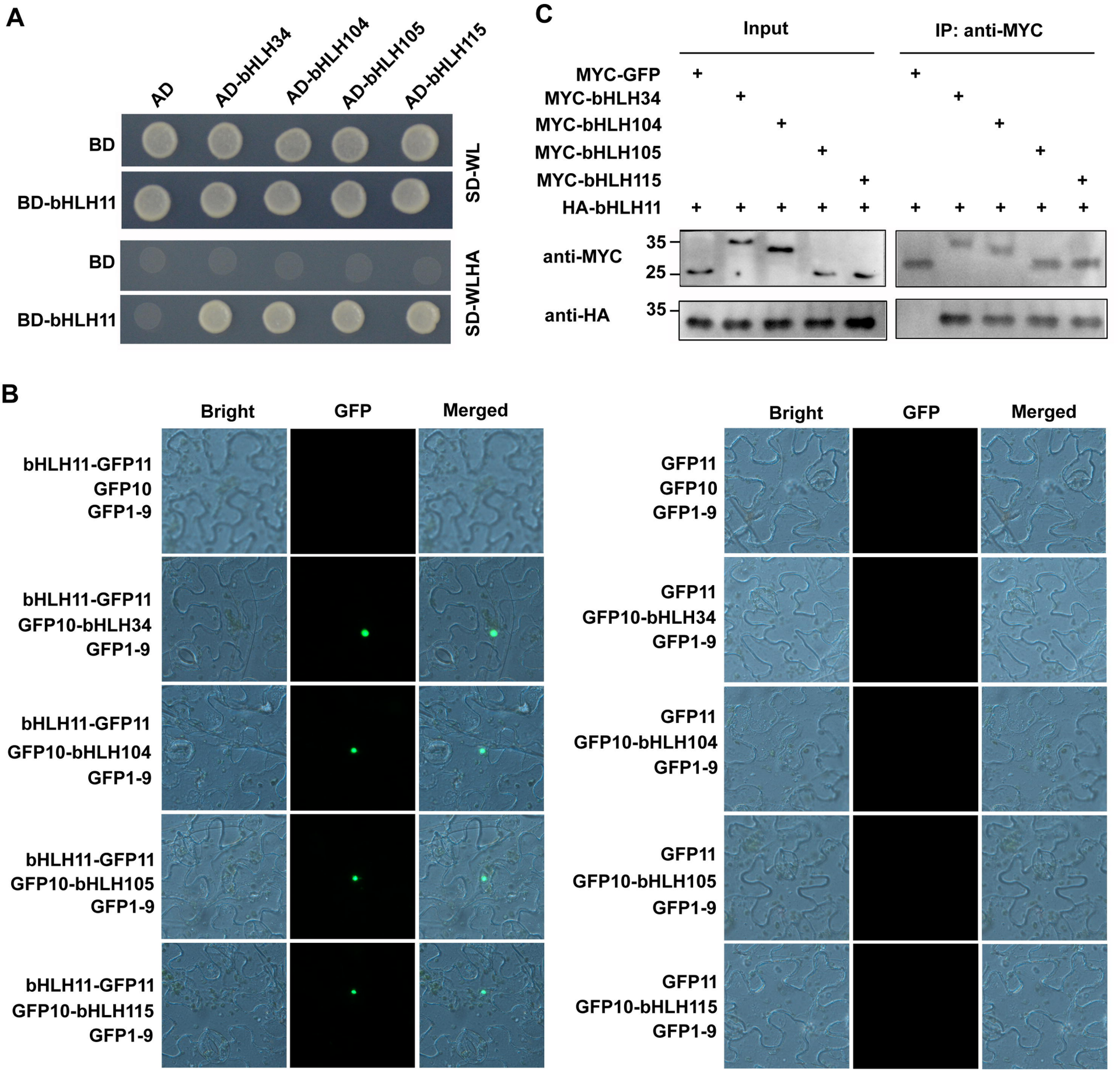
A
AD
AD-bHLH34
AD-bHLH104
AD-bHLH105
AD-bHLH115
BD
BD-bHLH11
SD-WL
BD
BD-bHLH11
SD-WLHA
C
Input
IP: anti-MYC
MYC-GFP
MYC-bHLH34
MYC-bHLH104
MYC-bHLH105
MYC-bHLH115
HA-bHLH11
anti-MYC
35
25
anti-HA
35
B
Bright
GFP
Merged
bHLH11-GFP11
GFP10
GFP1-9
bHLH11-GFP11
GFP10-bHLH34
GFP1-9
bHLH11-GFP11
GFP10-bHLH104
GFP1-9
bHLH11-GFP11
GFP10-bHLH105
GFP1-9
bHLH11-GFP11
GFP10-bHLH115
GFP1-9
Bright
GFP
Merged
GFP11
GFP10
GFP1-9
GFP11
GFP10-bHLH34
GFP1-9
GFP11
GFP10-bHLH104
GFP1-9
GFP11
GFP10-bHLH105
GFP1-9
GFP11
GFP10-bHLH115
GFP1-9

A

mCherry GFP Bright Merged

bHLH11-mCherry
GFP

bHLH11-mCherry
bHLH34-GFP

bHLH11-mCherry
bHLH104-GFP

bHLH11-mCherry
bHLH105-GFP

bHLH11-mCherry
bHLH115-GFP

B

Cytoplasm Nucleus

Fe0 Fe100 Fe300 Fe0 Fe100 Fe300

anti-HA

anti-HSP

anti-H3

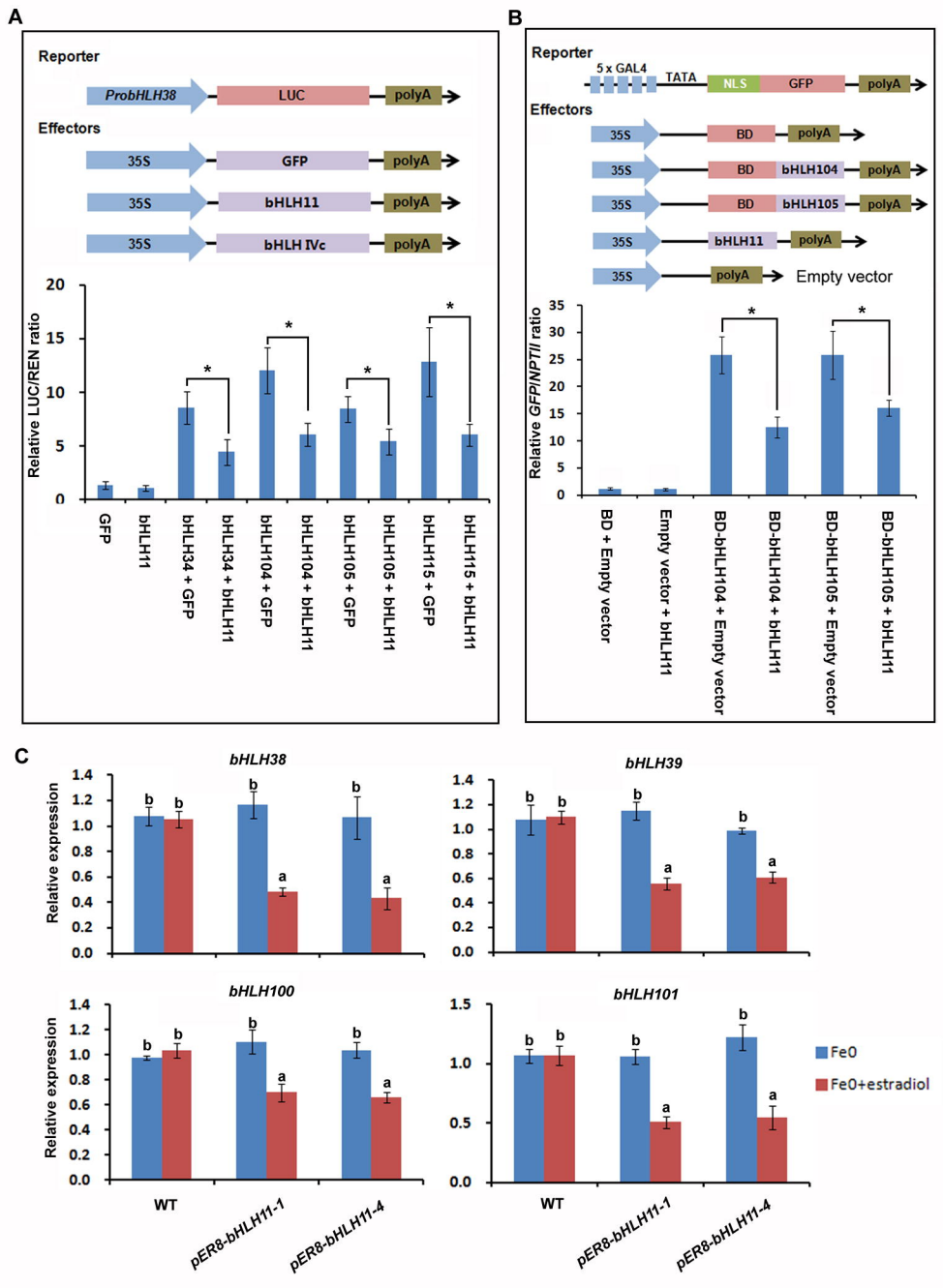
A
Reporter
ProbHLH38
LUC
polyA
Effectors
35S
GFP
polyA
35S
bHLH11
polyA
35S
bHLH IVc
polyA
Relative LUC/REN ratio
GFP
bHLH11
bHLH34 + GFP
bHLH34 + bHLH11
bHLH104 + GFP
bHLH104 + bHLH11
bHLH105 + GFP
bHLH105 + bHLH11
bHLH115 + GFP
bHLH115 + bHLH11
B
Reporter
5 x GAL4
TATA
NLS
GFP
polyA
Effectors
35S
BD
polyA
35S
BD
bHLH104
polyA
35S
BD
bHLH105
polyA
35S
bHLH11
polyA
35S
polyA
Empty vector
Relative GFP/NPTII ratio
BD + Empty vector
Empty vector + bHLH11
BD-bHLH104 + Empty vector
BD-bHLH104 + bHLH11
BD-bHLH105 + Empty vector
BD-bHLH105 + bHLH11
C
bHLH38
bHLH39
bHLH100
bHLH101
Relative expression
Fe0
Fe0+estradiol
WT
pER8-bHLH11-1
pER8-bHLH11-4

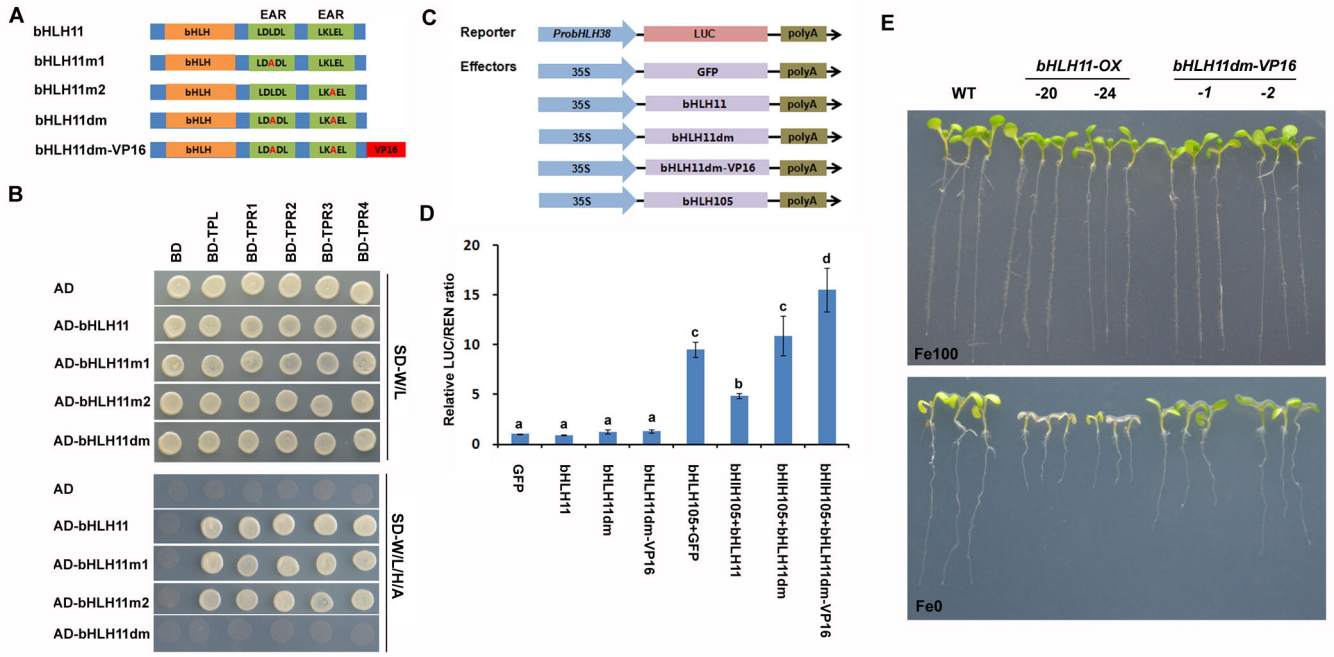
A
EAR
EAR
bHLH11
bHLH
LDLDL
LKLEL
bHLH11m1
bHLH
LDADL
LKLEL
bHLH11m2
bHLH
LDLDL
LKAEL
bHLH11dm
bHLH
LDADL
LKAEL
bHLH11dm-VP16
bHLH
LDADL
LKAEL
VP16
B
BD
BD-TPL
BD-TPR1
BD-TPR2
BD-TPR3
BD-TPR4
AD
AD-bHLH11
AD-bHLH11m1
AD-bHLH11m2
AD-bHLH11dm
SD-W/L
AD
AD-bHLH11
AD-bHLH11m1
AD-bHLH11m2
AD-bHLH11dm
SD-W/L/H/A
C
Reporter
ProbHLH38
LUC
polyA
Effectors
35S
GFP
polyA
35S
bHLH11
polyA
35S
bHLH11dm
polyA
35S
bHLH11dm-VP16
polyA
35S
bHLH105
polyA
D
Relative LUC/REN ratio
20
15
10
5
0
a
a
a
a
c
b
c
d
GFP
bHLH11
bHLH11dm
bHLH11dm-VP16
bHLH105+GFP
bHLH105+bHLH11
bHLH105+bHLH11dm
bHLH105+bHLH11dm-VP16
E
WT
bHLH11-OX
-20
-24
bHLH11dm-VP16
-1
-2
Fe100
Fe0

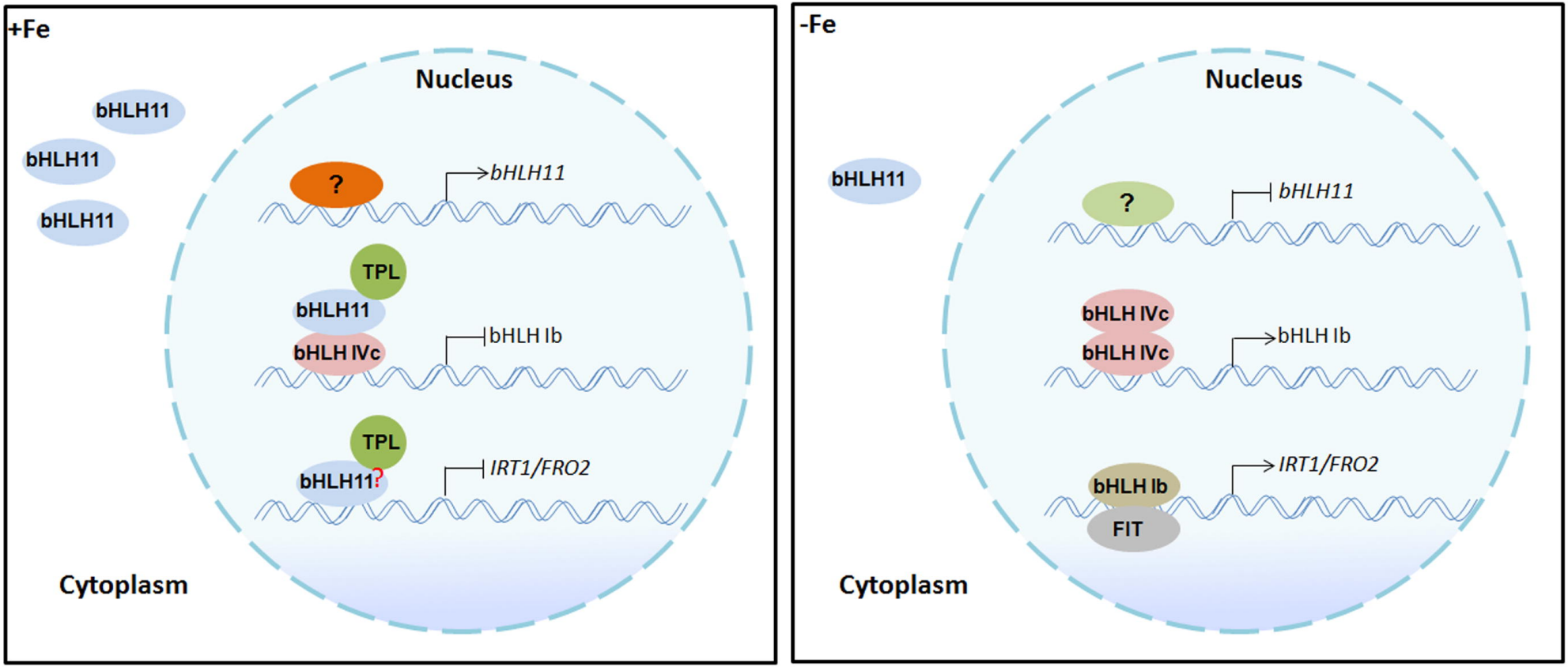
+Fe
Nucleus
bHLH11
bHLH11
bHLH11
?
bHLH11
TPL
bHLH11
bHLH IVc
bHLH Ib
TPL
bHLH11?
IRT1/FRO2
Cytoplasm
-Fe
Nucleus
bHLH11
?
bHLH11
bHLH IVc
bHLH IVc
bHLH Ib
bHLH Ib
FIT
IRT1/FRO2
Cytoplasm